Hindawi
Mathematical Problems in Engineering
Volume 2019, Article ID 5431047, 10 pages
https://doi.org/10.1155/2019/5431047

Research Article

Effect of Velocity Slip on Head Prediction for Centrifugal Pumps as Turbines

Xiaohui Wang, Junhu Yang, Zhengting Xia, Yan Hao, and Xiaorui Cheng

School of Energy and Power Engineering, Lanzhou University of Technology, Lanzhou 730050, China

Correspondence should be addressed to Junhu Yang; lzyangjh@lut.cn

Received 22 December 2018; Accepted 4 March 2019; Published 24 March 2019

Academic Editor: Changzhi Wu

The application of pumps as turbines (PAT) has been developed in several applications for energy recovery schemes. Therefore, establishing a performance correlation between pump mode and turbine mode is essential for selecting the proper machine. However, slip phenomenon is the challenges of head prediction for PAT. In this paper, the slip phenomenon of pump and PAT was revealed, and the slip factor was studied using CFD. The effect of slip on head prediction for PAT was analyzed, and a theoretical prediction model was presented considering slip factors. In order to validate the head prediction model, six centrifugal pumps with specific speed (n_s) from 9 to 54.8 were tested as turbines. Results showed that the predicted head by the proposed method was in good agreement with the experimental data, and it is more accurate than Stepanoff, Alatorre-Frenk, Sharma, and Derakhshan models. This method can be applied in head prediction for low specific speed PAT (n_s <60).

1. Introduction

Centrifugal pumps operating as turbines (PAT) are an attractive and important alternative for energy recovery solution. The use of PAT has been adapted in remote area power supply installations, as well as industrial application in energy recovery systems. Compared with traditional micro-hydro turbines, the PAT is a relatively simple machine, available for a wide range of heads and flows, easy to maintain, and readily available all over the world [1].

In recent studies, researches have attempted to build a model that would make accurate predictions of the turbine operation of pumps at best efficiency points (BEP). There have been several prediction techniques published so far, as reported by Stepanoff [2], Alatorre-Frenk [3], Sharma [4], Williams [5], Singh [6], Derakhshan, and Nourbakhsh [7, 8], Wang [9], and Ramos [10]. Most of these studies have suggested the relations for prediction of PAT behavior either based on efficiency or based on specific speed in pump mode, and a few have also derived the relations based on experimentation. However, the results obtained from these studies had an approximately ±20% deviation from experimental data [5], with deviations exceeding over 40% for some specific speeds [11]. One major reason for this was the slip phenomenon in turbine mode has not been considered, which has prevented an accurate performance prediction of PAT [12].

Slip phenomenon is known to strongly affect the performance of PAT, especially at off-design condition; it is usually considered as an important factor in the design process of turbo-machines (pump, compressor, or turbine) [13, 14]. In order to predict the performance characteristics, velocity slip within flow passages should be considered both in pump and in turbine modes, and the slip factor was calculated by means of numerical simulation in their papers [15, 16]. When a pump is running as a turbine, because of the velocity slip within impeller flow passages, the theoretical head of turbine is lower than Euler head, where the Euler head was obtained based on the infinite-blade hypothesis. Velocity slip should be taken into account accurately for head prediction of PAT. As a consequence, it is important to investigate slip factor and reveal the effect of slip on head prediction for PAT.

In order to overcome the challenges of head prediction for PAT, the velocity slip of PAT was researched and slip factor was calculated. Then a new head prediction model is proposed in consideration of slip factor in pump and turbine mode. Six centrifugal pumps with specific speed (n_s) from 9 to 54.8 were tested as turbines, and the head of the proposed

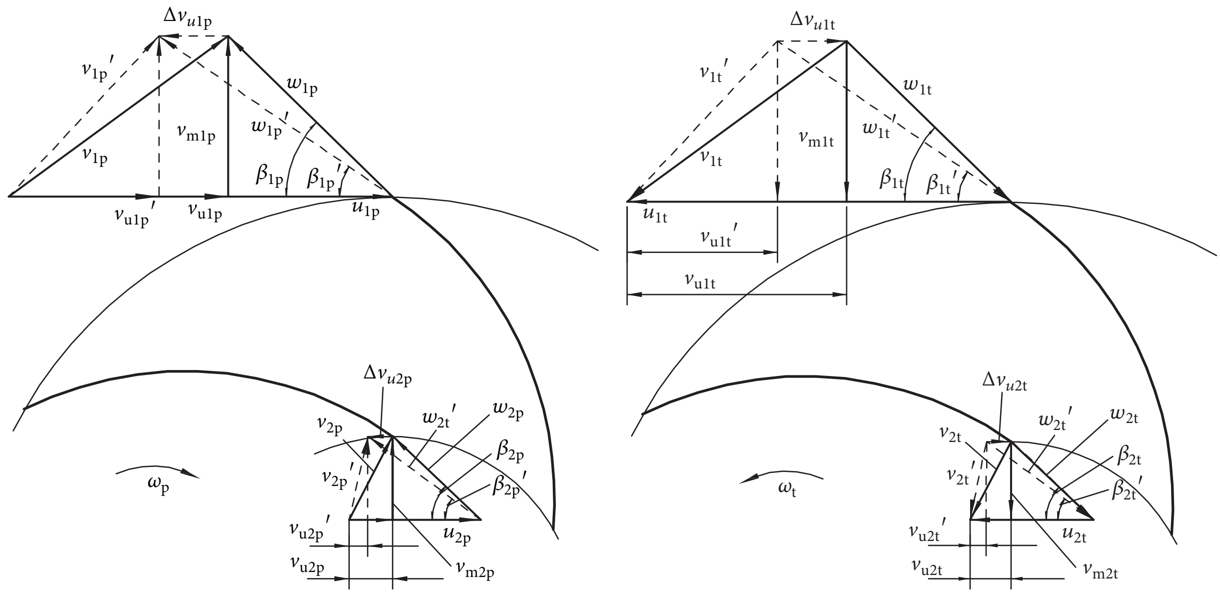

(a) Pump mode (b) Turbine mode

Figure 1: Velocity triangle of impeller.

model was compared with Stepanoff [2], Alatorre-Frenk [3], Sharma [4], and Derakhshan [8] methods. Deviations from experimental data are presented.

2. Theoretical Analysis

When a centrifugal pump operates as a turbine, flow and rotating directions are reverse. The velocity distribution within the impeller is shown in Figure 1 and heavy triangles are based on theoretical blade-to-blade analysis (Euler infinite-blade assumption), while dashed triangles are realistic velocity, where subscripts 1 and 2 refer to the high pressure side and low pressure side of the blade, respectively.

Due to the fact that the blades of PAT are always finite, the realistic flow in impeller passage is produced by axial-eddy and through flow [17, 18], which causes a difference between the flow angle β' and the blade angle β. This angular difference corresponds to an absolute-tangential velocity difference Δv_u (Figure 1). This is known as slip velocity, which is different in pump mode and turbine mode. For pump, the relative velocity at the outlet (high pressure side) of impeller does not match the blade surface, inducing slip velocity Δv_{u1}, when a pump runs as turbine. Similarly, the slip velocity occurs at the inlet of impeller, as shown in Figure 2. Additionally, slip velocity also exists at pump blade inlet and turbine blade outlet, but it was neglected in this paper since the Δv_{u2} is very small. The slip velocity induces the change of v_{u1}, which causes the theoretical head of impeller to be smaller than Euler head. Therefore, slip phenomenon should be considered for head prediction of PAT.

If the rotational speeds are the same, there are equal and opposite heavy line velocities for pump mode and turbine

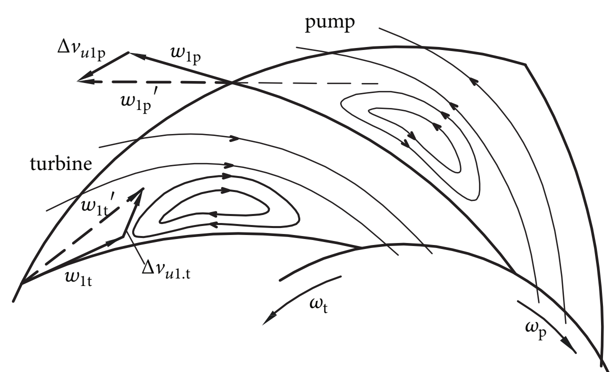

Figure 2: Slip phenomenon for pump and turbine modes.

modes based on the infinite-blade theory. Consequently, Euler head in pump and turbine mode are the same

$$H_{Euler} = \frac{u_1 v_{u1} - u_2 v_{u2}}{g} \tag{1}$$

where u is peripheral speed, v_u is peripheral component of velocity, g is gravitational acceleration, and subscripts 1 and 2 devote the high pressure side and low pressure side of the blade, respectively.

In (1), v_{u2} is negligibly small in general; as a result, the Euler head can be as

$$H_{\text{Euler}} = \frac{u_1 v_{u1}}{g} \tag{2}$$

where u_1 and v_{u1} can be obtained depend on the velocity triangle as shown in Figure 1(b) with heavy line,

$$u_1 = \frac{\pi n D_1}{60} \tag{3}$$

$$v_{u1} = u_1 - \frac{Q}{\pi D_1 b_1} \cot \beta_{b1} \tag{4}$$

where n is impeller rotational speed, D is impeller diameter, b is flow passage width, β_b is blade angle, and Q is flow rate.

Because of the finite-blade of impeller, the theoretical head H_{th} of impeller is difficult to obtained by theoretical method, which can be predicted by CFD as follows:

For pump mode

$$H_{th.p} = \frac{H_p}{\eta_{hp}} \tag{5}$$

For turbine mode

$$H_{th.t} = H_t \cdot \eta_{ht} \tag{6}$$

where H is net head and η_h is hydraulic efficiency of impeller.

Therefore, the head reduction ΔH caused by slip velocity for pump mode and turbine mode is

$$\Delta H_p = H_{Euler} - H_{th.p} \tag{7}$$

$$\Delta H_t = H_{Euler} - H_{th.t} \tag{8}$$

Then, the slip factor of pump and PAT can be described as

$$s_p = \frac{\Delta H_p}{H_{Euler}} \tag{9}$$

$$s_t = \frac{\Delta H_t}{H_{Euler}} \tag{10}$$

As mentioned above, the Euler head H_{Euler} can be calculated using (1); theoretical head H_{th} can be obtained by Computational Fluid Dynamics (CFD) methodology; as a result, the slip factor was acquired by (9) and (10).

In this paper, the slip factor of pump and turbine modes was studied. The effect of velocity slip on head prediction of PAT was analyzed, and a prediction model was presented. Finally, an experiment was performed to verify the prediction model.

3. Numerical Investigation

3.1. Numerical Simulation. In the present work, CFD was used for numerical research of PAT. Considering the Direct Numerical Simulation (DNS) is out of range due to the high computer power needed, and Large Eddy Simulation (LES) is currently only feasible for simplified pump elements [19], the computations were performed by means of the Reynolds Average Navier-Stokes (RANS) equations with an appropriate turbulence model. In this study, the ANSYS-CFX was selected for the solution of the steady 3D Navier-Stokes equation. There are many turbulence models in use today, and four of the most popular turbulence models are the standard k-ε, RNG k-ε, standard k-ω, and SST k-ω model. In the attempt to adopt the most appropriate turbulence model for solving RANS equations, these four models were applied, respectively, for PAT performance simulation. The head of PAT calculated by these four models and experiment data was compared, and the most accurate one was chosen.

Table 1: The main geometric parameters of PAT.

	category	parameter
Impeller	D_1(mm)	312
	D_2(mm)	80
	d_h(mm)	0
	b_1(mm)	10
	β_1(°)	32
	Z	6
	θ(°)	150
Volute	D_{in} (mm)	50
	b_0 (mm)	24
	D_0 (mm)	320
Draft tube	D_{out} (mm)	80

Table 2: Range of Y+ for near-wall mesh.

	Standard k-ε	RNG k-ε	Standard k-ω	SST k-ω
Volute	7.6~184.2	7.6~184.2	5.2~87.5	5.2~87.5
Impeller	3.7~194.3	3.7~194.3	2.3~98.7	2.3~98.7
Draft tube	26.3~31.4	26.3~31.4	26.3~31.4	26.3~31.4

A centrifugal pump with specific speed 9.0 is operating as a turbine for numerical simulation (Figure 3). The head, discharge, and rotational speed of selected pump were 32 m, 25m^3/h, and 1,450 rpm, respectively. Table 1 gives the main geometry parameters of the PAT. The 3D model of this PAT was generated including the volute, impeller, and draft tube.

Considering the numerical simulation converges more rapidly and accurately by utilizing structure grid, an ICEM-CFD was used to generate a pure hexahedral grid for each component part of simulated domain (Figure 4). The different y+ should be satisfied for different turbulence models. For the k-ε turbulence model, a near wall result must be obtained using scalable wall function, for a y+ near 200, while y+ ≤100 was appropriate for the k-ω model with automatic wall function [20]. The range of y+ for near wall is provided in Table 2.

A grid sensitivity analysis was performed to verify the grid-independence of results. It was found that when the grid element was beyond 4×10^6, the heads of PAT were almost constant regardless of using standard k-ε, RNG k-ε, standard k-ω, and SST k-ω model (Figure 5). The final elements number of fluid volume was 4,154,084.

3.2. Validation of Numerical Simulation. The PAT was simulated and the results were compared with experimental data.

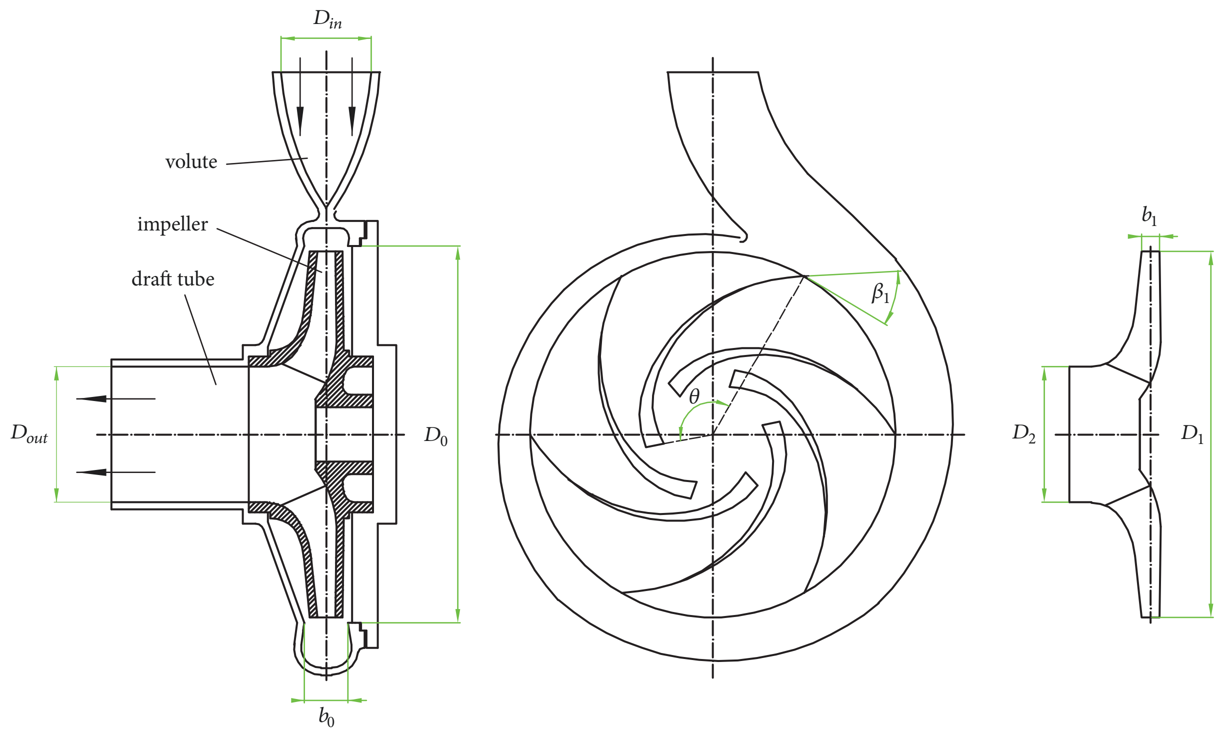

Figure 3: The geometrical model of PAT.

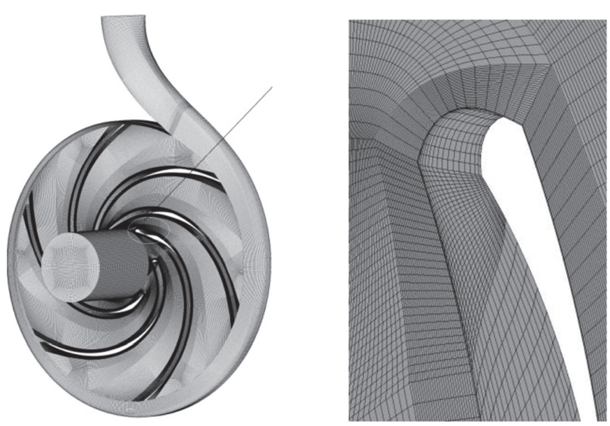

Figure 4: Structured grid of PAT.

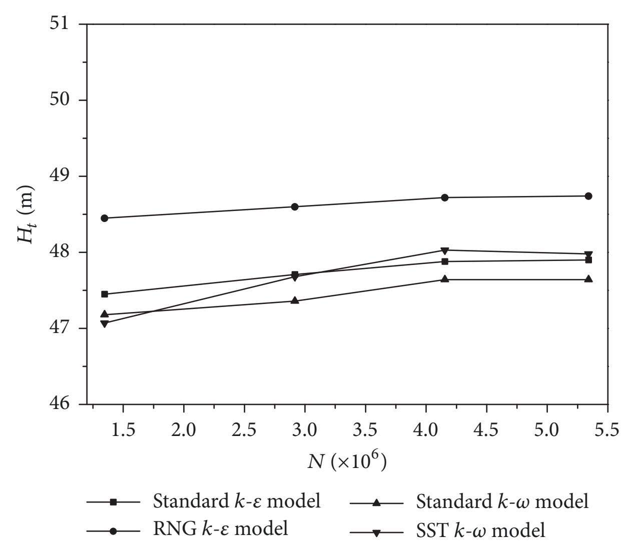

Figure 5: Grid independent test.

The experimental test rig was showed in Figure 6. A feed pump was installed to provide the pressure flow for PAT, and another pump was connected to PAT shaft for consuming the energy generated by PAT. A flow regulating valve was installed at outlet pipe of consume pump for keeping the rotational speed. Two pressure transmitters ABG-M2 with range of 0-2MPa were set at the inlet and outlet of PAT, respectively, for measuring pressure, an electromagnetic flow meter MF200-101 was set at the inlet pipe of PAT for measuring the discharge, and a NJ1 torque meter was installed at PAT shaft for measuring the rotational speed and torque of PAT. The discharge, head, shaft power, and efficiency of PAT were calculated after all parameters were measured. The uncertainty in different performance parameters was estimated in accordance with the procedure as described by Moffat [21]. The relative uncertainty in discharge, head, shaft power, and efficiency of PAT were ±0.82%, ±1.2%, ±1.72%, and ±2.5%, respectively.

Simulation using four turbulence models mentioned above was done for tested PAT, and the validation results were shown in Figure 7. CFD could not simulate disc friction, mechanical losses, and leakage since the flow volume did not include the space between impeller hub/shroud and casing

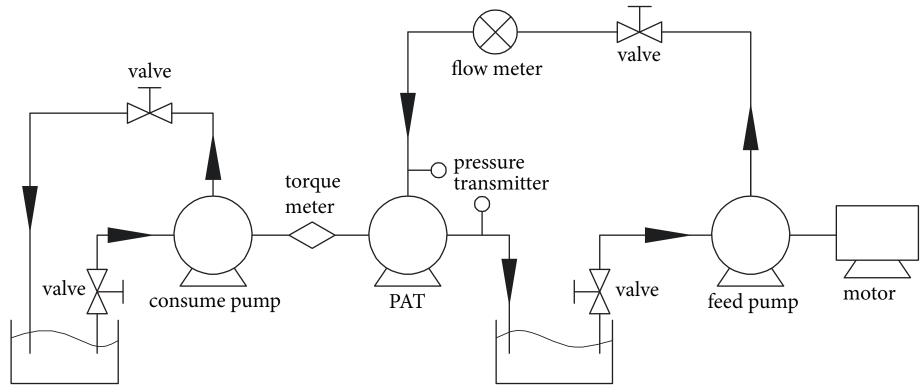

(a) Schematic diagram of experimental test rig

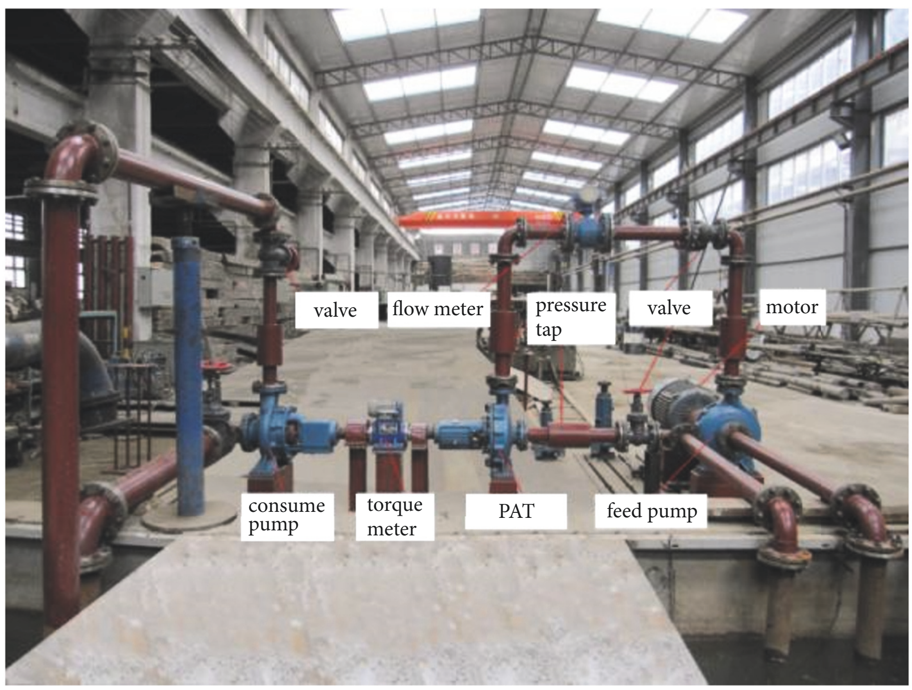

(b) Test rig of PAT

Figure 6

or the sealing gap. Despite the loss generated in experiment of PAT, the PAT need more head to overcome the loss reasonably. As a result, the head of PAT predicted by CFD was slightly lower than the experimental result. This was confirmed by other papers [7, 22].

Here, Φ and Ψ are flow rate and head coefficient, respectively, which can be defined as

$$\phi = \frac{Q}{nD_1^3} \tag{11}$$

$$\psi = \frac{gH}{n^2D_1^2} \tag{12}$$

The results showed that the mean deviations of standard k-ε, RNG k-ε, standard k-ω, and SST k-ω model from the experimental result were 6.62%, 5.53%, 7.82%, and 6.46%, while the mean-square deviations were 0.63%, 0.33%, 0.56%, and 1.65%, respectively. It can be seen that the minimum deviation was the RNG k-ε model. Therefore, the RNG k-ε model confirms a good accuracy in the performance prediction of PAT; it was adopted for head prediction in this paper.

4. Results and Discussion

4.1. Slip Phenomenon in Pump and PAT. Figure 8 gives the streamline of pump and PAT at best efficiency point; it can be seen that axial vortex occurred within flow passages. As predicted in Figure 2, the relative velocity did not match to the blade surface owing to the flow slip and the axial vortex was derived near the pressure side of blade. The vortex direction was opposite to impeller rotation, and the vortex structure and position were different for pump and PAT; it

Table 3: Geometric parameters of PATs.

n_s	Impeller parameters					Volute parameters		
	D_1(mm)	D_2(mm)	b_1(mm)	β_{b1}(°)	θ(°)	D_0(mm)	b_0(mm)	D_{in}(mm)
9.0	312	80	10	32	150	320	24	80
15.1	272	98	10	32	138	280	26	80
23.6	210	90	16	26	134	220	36	65
35.1	216	125	26.5	17/22	107	230	42	100
49.3	143	86	24	29	86	160	40	80
54.8	246	157	39	26	100	256	60	200

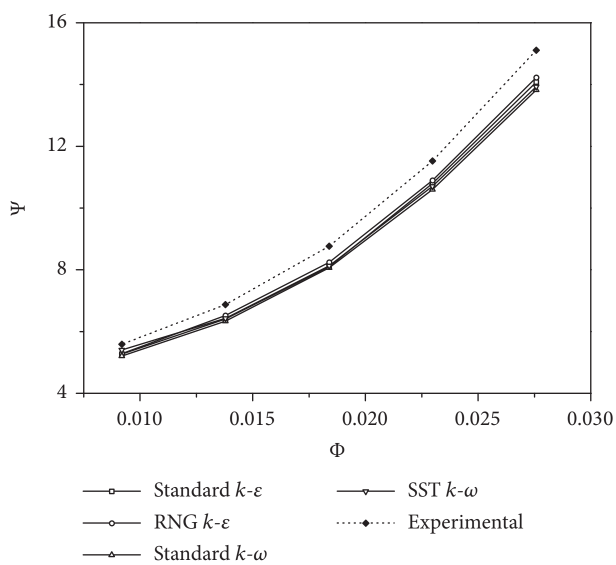

Figure 7: CFD and experimental results of PAT.

occurred next to the center of blade and was surrounded with main flow for pump and occurred near the outlet of blade for PAT.

The uniform flow distribution would be induced by axial vortex, which influences the energy transformation of blades reasonably. Figure 9 gives the relative velocity distribution on the blade of pump and PAT. It was observed that the relative velocity increased uniformly along the blade of suction side for both pump and PAT, and humped (increased and then decreased) for pressure side, which was caused by slip phenomenon within flow passages. The bad velocity distribution leads to the pressure fluctuate on the blade, as shown in Figure 10. The pressure distribution of pump was more uniform than PAT since the vortex was surrounded and difficult to spread; however, pressure fluctuations can be observed near the outlet of blade for PAT due to the unstable vortex, which was derived next to blade outlet and interacted with flow in volute. Additionally, the nonuniform velocity distribution in flow passage induces the friction of adjacent flow particle, which leads to the additional hydraulic loss.

Slip phenomenon induces the axial vortex next to the blade surface, the vortex regions are always the low pressure region, and additionally, pressure fluctuation can be observed. As a consequence, the energy transformed between fluid and blade is reduced in these regions, the theoretical head smaller than Euler head positively. This phenomenon exists both in pump and in PAT, but its behavior is different from each other. Therefore, the slip phenomenon should be considered in performance prediction of PAT.

4.2. Slip Factor. The slip factor of pump and PAT is different due to opposite flows. It is of interest to investigate the slip phenomenon and to obtain the effective value of slip factor of pump and turbine mode. As mentioned in (7)–(10), the slip factor is related to the Euler head and the theoretical head. The Euler head was obtained by theoretical calculation using (1) for each PAT, and the theoretical head was achieved using CFD simulation in this paper. As a result, the slip factor was obtained.

Figure 11 shows the slip factor and hydraulic efficiency for pump mode and turbine mode of PAT in all examined conditions. It was observed that the slip factors of pump and turbine modes were different in both design condition and off-design condition. The slip factor increased with flow rate in pump operation and decreased in turbine operation. The value approached 0.28 at BEP for pump mode and 0.24 for turbine mode. It rose dramatically at low flow rate of turbine mode, and turbine efficiency decreased similarly. The larger the S value, the more serious the slip. From the theoretical point of view, slip phenomenon induces additional hydraulic loss in impeller passage of PAT. The slip phenomenon strengthened in part-load region; thus the hydraulic efficiency was relatively low. On the contrary, the slip phenomenon weakened in the over load region, so the hydraulic efficiency of PAT was relatively high. This is also a reason why PAT's efficiency is higher in large flow rate. Therefore, when a centrifugal pump runs as a turbine, it is not recommended for the machine to work at a low flow rate.

For investigating the slip factor of pump and turbine modes at BEP, six centrifugal pumps with specific speeds from 9 to 54.8 were selected. The geometric parameters of these pumps are shown in Table 3. Figure 12 shows that the slip factor varied with different specific speed of PAT, and it was higher in pump mode than turbine mode at BEP; the hydraulic efficiency of the pump mode was lower than turbine mode.

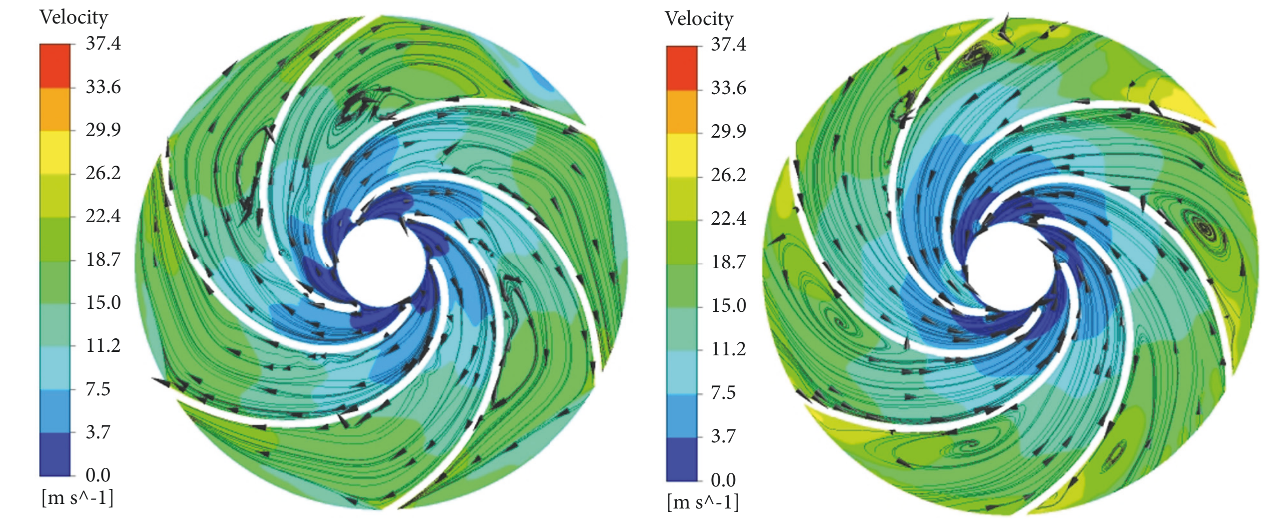

(a) Pump mode (b) Turbine mode

Figure 8: Streamline of impeller flow.

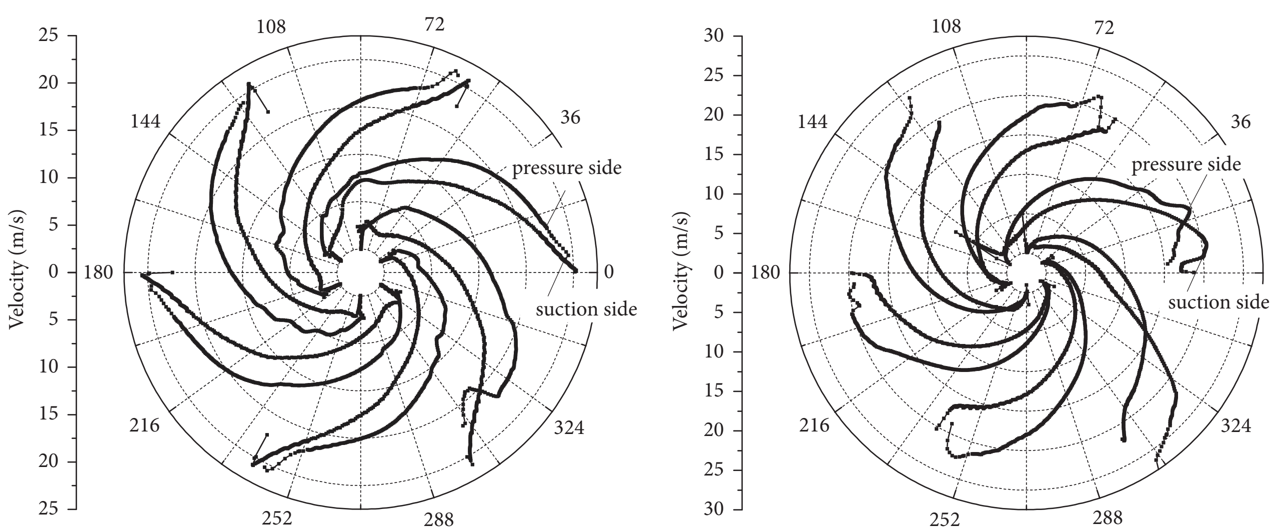

(a) Pump mode (b) Turbine mode

Figure 9: Relative velocity distribution of PAT impeller.

4.3. Performance Prediction of PAT. Using (5)–(10), the net head of pump and PAT can be described as

$$H_p = \eta_{hp} \cdot \left(1 - s_p\right) \cdot H_{\text{Euler}} \tag{13}$$

$$H_t = \frac{\left(1 - s_t\right) \cdot H_{\text{Euler}}}{\eta_{ht}} \tag{14}$$

Therefore, at the same rotational speed, the head correlation between pump and PAT is

$$\frac{H_t}{H_p} = \frac{1 - s_t}{1 - s_p} \frac{1}{\eta_{ht} \eta_{hp}} \tag{15}$$

Six industrial centrifugal pumps with specific speeds from 9 to 54.8 were tested and the results are shown in Table 4. The predictions obtained by Stepanoff, Alatorre-Frenk, Sharma, Derakhshan, and the proposed method are listed in the table for comparison.

Figure 13 shows the deviations of these methods from the experimental data. The slip phenomenon was considered in the proposed new method of head prediction; it can be seen that the mean deviations of predicted head correlation by Stepanoff, Alatorre-Frenk, Sharma, Derakhshan and the suggested new method were 8.60%, 16.72%, 15.23%, 13.83%, and 5.70% from experimental data, respectively. The results showed that the proposed method had the minimum mean deviation, which means this method closely resembles the experimental result. Thus it can be considered that the proposed method is more accurate for PAT with $9 < n_s < 54.8$ than the others. This method can be

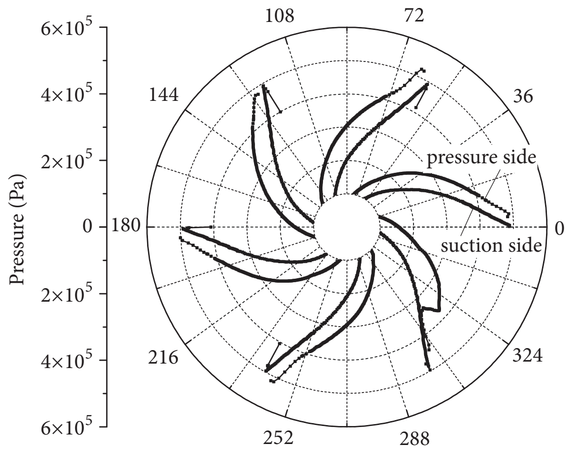

(a) Pump mode

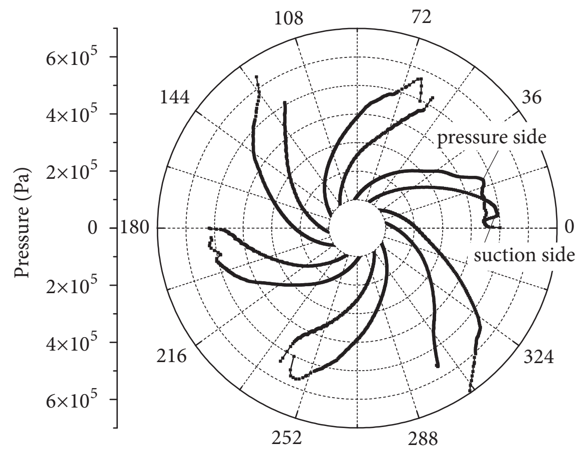

(b) Turbine mode

FIGURE 10: Pressure distribution of PAT impeller.

TABLE 4: Head correlations between pump and PAT.

n_s	H_t/H_p					
	Stepanoff	Alatorr-Frenk	Sharma	Derakhshan	New method	Experimental data
9.0	1.42	2.32	2.01	1.93	1.58	1.55
15.1	1.98	1.93	1.56	2.04	1.81	1.63
23.6	1.72	1.47	1.29	1.83	1.49	1.54
35.1	1.62	1.41	1.26	1.64	1.47	1.60
49.3	1.70	1.31	1.22	1.45	1.61	1.53
54.8	1.40	1.22	1.17	1.38	1.52	1.48

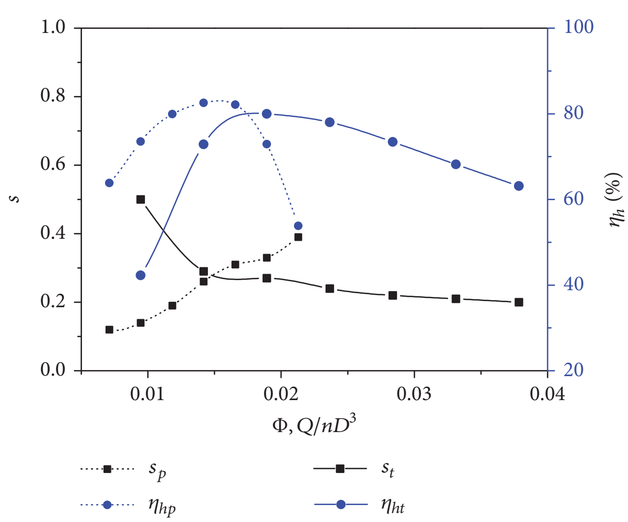

FIGURE 11: Slip factor and efficiency curves of PAT.

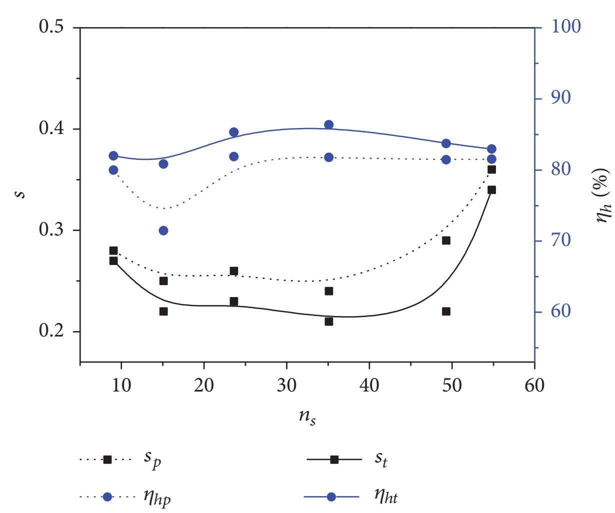

FIGURE 12: Slip factor and hydraulic efficiency curves.

applied in performance prediction for pump operating as turbine.

5. Conclusion

In the present study, the velocity slip of pump and PAT was revealed, and the slip factor was studied using CFD. The effect of velocity slip on head prediction for PAT was analyzed, and a theoretical prediction model was presented considering slip factors. Finally, an experiment was performed to verify the prediction model. The results showed that the slip factor of pump was higher than PAT at BEP. However, the hydraulic efficiency was smaller at BEP.

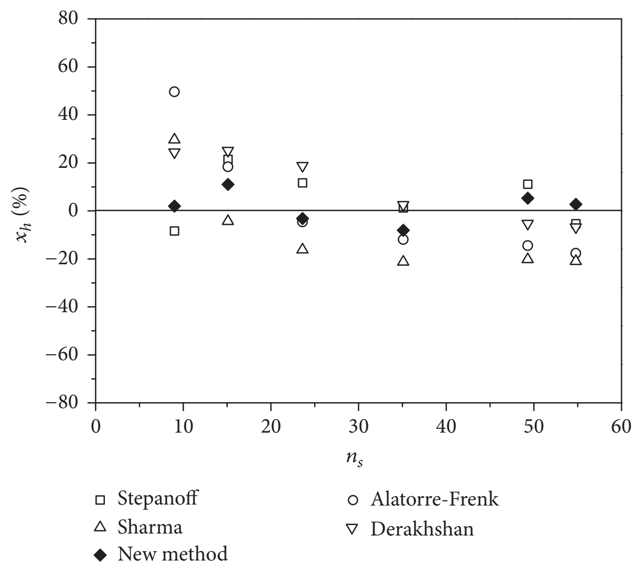

FIGURE 13: Head deviations based on experimental data.

Six centrifugal pumps with specific speed from 9 to 54.8 were tested as turbines. Results showed that the predicted head by the proposed method was in good agreement with the experimental data. Additionally, the predictions of the proposed method were more accurate than the predictions of Stepanoff, Alatorre-Frenk, Sharma, and Derakhshan models for PAT with $9 < n_s < 54.8$.

Nomenclature

b: Flow passage width, m
D: Diameter, m
d_h: Hub diameter, m
Z: Blade number
g: Gravitational acceleration, m/s^2
Q: Flow rate, m^3/s
Q_d: Flow rate at design-point, m^3/s
H: Head, m
ΔH: Hydraulic loss head, m
N: Mesh number
n: Rotate speed, rpm
n_s: Specific speed, $n_s = (n,\text{rpm})(Q,\text{m}^3/\text{s})^{1/2}/(H,\text{m})^{3/4}$
v: Absolute velocity, m/s
w: Relative velocity, m/s
u: Peripheral velocity, m/s
v_u: Peripheral component of velocity, m/s
v_m: Meridian component of velocity, m/s
Δv_u: Slip velocity, m/s
x: Deviation, %
s: Slip factor.

Greek Symbols

β': Relative flow angle [°]
β: Blade inlet angle [°]
θ: Blade wrap angle [°]
ω: Rotate angle speed [rad/s]
Φ: Discharge number
Ψ: Head number
η_h: Hydraulic efficiency [%].

Superscript

$'$: Infinite-blade assumption.

Subscripts

p: Pump
t: PAT
th: Theoretical
0: Volute
1: High pressure side
2: Low pressure side
h: Head ratio.

Data Availability

The data used to support the findings of this study are available from the corresponding author upon request.

Conflicts of Interest

The authors declare that they have no conflicts of interest.

Acknowledgments

This work is supported by Nature Science Foundation of China (51569013); Youth Science and Technology Foundation Plan of Gansu (145RJYA312).

References

[1] D. R. Giosio, A. D. Henderson, J. M. Walker, P. A. Brandner, J. E. Sargison, and P. Gautam, "Design and performance evaluation of a pump-as-turbine micro-hydro test facility with incorporated inlet flow control," *Journal of Renewable Energy*, vol. 78, pp. 1–6, 2015.

[2] A. J. Stepanoff, *Centrifugal and Axial Flow Pumps, Design and Applications*, John Wiley and Sons, NY, 1957.

[3] C. Alatorre-Frenk, *Cost Minimization in Microhydro Systems Using Pumps-as-Turbines*, University of Warwick, 1994.

[4] K. Sharma, "Small hydroelectric project-use of centrifugal pumps as turbines," Tech. Rep., Kirloskan Electric Company, Bangalore, India, 1985.

[5] A. Williams, *Pumps as Turbines Users Guide*, International Technology Publications, London, 1995.

[6] P. Singh and F. Nestmann, "A consolidated model for the turbine operation of centrifugal pumps," *Journal of Engineering for Gas Turbines and Power*, vol. 133, pp. 1–9, 2011.

[7] S. Derakhshan and A. Nourbakhsh, "Theoretical, numerical and experimental investigation of centrifugal pumps in reverse operation," *Experimental Thermal and Fluid Science*, vol. 32, no. 8, pp. 1620–1627, 2008.

[8] S. Derakhshan and A. Nourbakhsh, "Experimental study of characteristic curves of centrifugal pumps working as turbines

in different specific speeds," *Experimental Thermal and Fluid Science*, vol. 32, no. 3, pp. 800–807, 2008.

[9] X. H. Wang, J. H. Yang, and F. X. Shi, "Theoretical and numerical study of performance prediction of centrifugal pump as turbine," *Applied Mechanics and Materials*, vol. 444, pp. 579–587, 2014.

[10] H. Ramos and A. Borga, "Pumps as turbines: an unconventional solution to energy production," *Urban Water Journal*, vol. 1, no. 3, pp. 261–263, 1999.

[11] P. Singh and F. Nestmann, "An optimization routine on a prediction and selection model for the turbine operation of centrifugal pumps," *Experimental Thermal and Fluid Science*, vol. 34, no. 2, pp. 152–164, 2010.

[12] X. H. Wang, J. H. Yang, and Z. T. Xia, "Study on slip phenomenon of pumps as turbines in different working conditions," in *Proceedings of the ASME 2017 Fluid Engineering Division Summer Meeting*, Waikoloa, Hawaii, USA, 2017.

[13] C. Pfleiderer, *Die Kreiselpumpen fur Flussigkeiten und Gase*, Chinese edition, translation from the 5th German edition by Q. D. Xi, 1983.

[14] C. Ji, J. Zou, X. D. Ruan, P. Dario, and X. Fu, "A new correlation for slip factor in radial and mixed-flow impellers," *Proceedings of the Institution of Mechanical Engineers, Part A: Journal of Power and Energy*, vol. 225, no. 1, pp. 114–119, 2011.

[15] G. Ardizzon and G. Pavesi, "Optimum incidence angle in centrifugal pumps and radial inflow turbines," *Proceedings of the Institution of Mechanical Engineers, Part A: Journal of Power and Energy*, vol. 212, no. 2, pp. 97–107, 1998.

[16] G. Ventrone, G. Ardizzon, and G. Pavesi, "Direct and reverse flow conditions in radial flow hydraulic turbomachines," *Proceedings of the Institution of Mechanical Engineers, Part A: Journal of Power and Energy*, vol. 214, no. 6, pp. 635–644, 2000.

[17] A. Busemann, "Das Förderhöhenverhältnis radialer Kreiselpumpen mit logarithmisch-spiraligen Schaufeln," *ZAMM - Zeitschrift für Angewandte Mathematik und Mechanik*, vol. 8, no. 5, pp. 372–384, 1928.

[18] G. F. Wislicenus, *Fluid Mechanics of Turbomachinery*, Dover Publications, NY, 2nd edition, 1965.

[19] J. C. Páscoa, F. J. Silva, J. S. Pinheiro, and D. J. Martins, "Accuracy details in realistic CFD modeling of an industrial centrifugal pump in direct and reverse modes," *Journal of Thermal Science*, vol. 19, no. 6, pp. 491–499, 2010.

[20] X. j. Li, S. Q. Yuan, and Z. Y. Pan, "Realization and application evaluation of near-wall mesh in centrifugal pumps," *Transactions of the Chinese Society of Agricultural Engineering*, vol. 28, pp. 67–72, 2012.

[21] R. J. Moffat, "Contributions to the theory of single-sample uncertainty analysis," *ASME Journal of Fluids and Engineering*, vol. 104, no. 2, pp. 250–258, 1982.

[22] A. Rodrigues, P. Singh, A. Williams, F. Nestmann, and E. Lai, "Hydraulic analysis of a pump as a turbine with CFD and experimental data," in *ImechE, Seminar Proc. Of Advances of CFD in Fluid Machinery Design*, London, England, 2003.

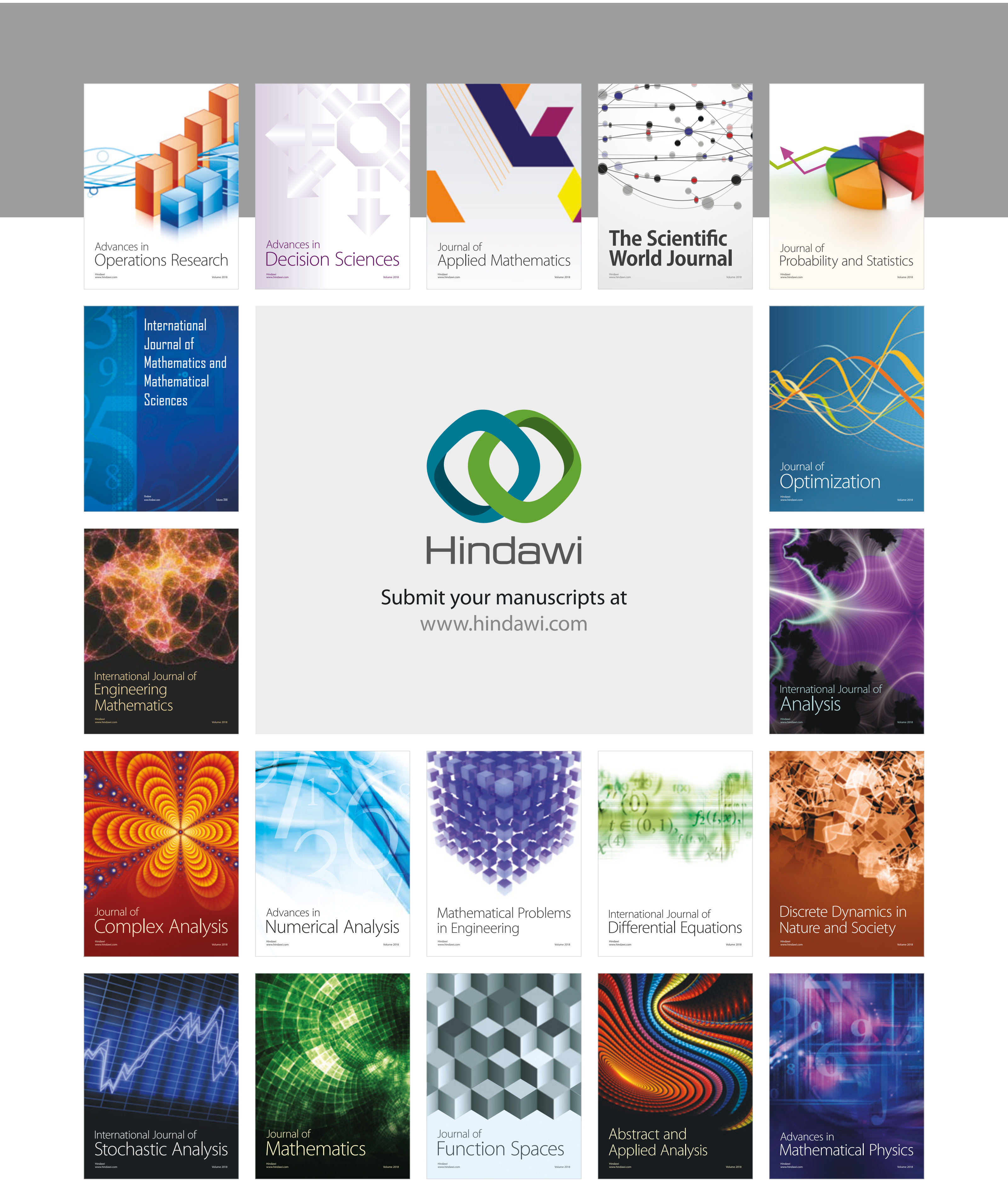
Advances in
Operations Research
Advances in
Decision Sciences
Journal of
Applied Mathematics
The Scientific
World Journal
Journal of
Probability and Statistics
International
Journal of
Mathematics and
Mathematical
Sciences
Hindawi
Submit your manuscripts at
www.hindawi.com
Journal of
Optimization
International Journal of
Engineering
Mathematics
International Journal of
Analysis
Journal of
Complex Analysis
Advances in
Numerical Analysis
Mathematical Problems
in Engineering
International Journal of
Differential Equations
Discrete Dynamics in
Nature and Society
International Journal of
Stochastic Analysis
Journal of
Mathematics
Journal of
Function Spaces
Abstract and
Applied Analysis
Advances in
Mathematical Physics